Impact of Time Delay Margin on the Stability of Load Frequency Systems with Electric Vehicle Aggregator

A. Jawahar[1*] ⓘD, K. Ramakrishnan[2]

[1, 2] Electrical and Electronics Engineering Department, Pondicherry Engineering College, Puducherry, India
E-mail: jawahar.a@pec.edu

Abstract— Open channel communication is a major prerequisite for next generation power networks in which time delays are inevitable. Due to unforeseen variations in the load demand, the mismatch between power generation and demand occurs. If this situation is not properly tackled, it may induce some unintended consequences like fluctuations in the tie-line power and system frequency which are highly undesirable. To ensure grid reliability, the frequency should always stay within its stipulated range. This is accomplished by load frequency control (LFC) technique. In networked LFC systems, load frequency regulation signals are transferred via communication networks, causing time delays in the feedback paths that can destabilize the power grid. As a consequence, for ensuring stability, the stable delay margin must, therefore, be determined. In this paper, the delay-dependent stability problem of two area LFC systems combined with electric vehicle aggregator (EVA) is addressed. The conducted Lyapunov based analysis yields a stable delay margin within which the closed loop system remains asymptotically stable. Moreover, the analytical delay margin values are validated using the simulation studies. In the sequel, the effect of participating factors on the system stability is also investigated.

Keywords— Load frequency control; Delay-dependent stability; Lyapunov-Krasovskii functional; Linear matrix inequality; Electric Vehicle Aggregator; Stability criterion.

1. INTRODUCTION

Load frequency control (LFC) is a control strategy employed in the power systems to ensure demand-generation balance at all times. The imbalance in demand-generation is indicated by an incremental change in the system frequency [1-4]. If the demand exceeds the generation, there is a fall in the system frequency from its equilibrium value and if the demand falls below generation, the system frequency shoots up. The main objective of the LFC system is to ensure a constant grid frequency in presence of continuous variations in the power system load. The LFC scheme, during load variation, processes the incremental frequency variable and delivers an appropriate command (control effort) to the governor. The governor, by manipulating the valve mechanism of the turbine, either increases or decreases the mechanical input to the synchronous generator and restores normalcy in the power system. By exercising such a control, an LFC system saves the alternator from going out of synchronism from the main grid. This in turn, ensures that the power grid stays healthy and robust [5-8].

The changing scenario and modernization of the conventional electric grid led to extensive penetration of renewable energy resources such as wind, PV, fuel cells, etc. The addition of these distributed generation units increases the complexity of the existing LFC system in terms of frequency regulation and stability issues. Along with integrating renewable energy resources, energy storage devices, which are brought into the system for improved frequency compensation, further complicate the above situation [9-13].

In the networked power system framework, the LFC is housed in a centralized control center that is geographically displaced from the generating station. A communication network is employed to facilitate the control and information exchange between the remote-control center and power plant [11-15]. Using a communication channel in the feedback loop introduces time-delay in the closed loop system. This inevitable loop delay has an adverse impact on the performance and stability of the closed loop system [16-22].

In dire situations, when the delay magnitude exceeds a critical margin called stable delay margin, the connected generator fails to operate in synchronism with the grid; eventually, the machine trips from the grid causing an unbalance in the power system. Hence, delay-dependent stability analysis is a procedure to assess the stable delay margin of proposed LFC scheme [23-27]. The computation of delay margin enables the operating personnel to achieve optimal performance from the system under varying load conditions. Owing to consistent fluctuations in power generation from environment dependent renewable energy sources, the frequency regulation and stability of power system gets affected [28-32]. With the ability to quickly modify the output power from energy storage systems like batteries and the use of vehicle-to-grid technologies, electric vehicles (EVs) have emerged as a viable tool for minimizing the intermittent impacts of renewable energy sources and regulating the frequency of the power grid. The rapid responsiveness of EVs substantially contributes to the improvement of the dynamic performance of LFC systems. Since EVs can be used as either loads or generators, they can compensate for the fluctuations; as a result, they enhance the frequency stability of the system. In addition, numerous time domain techniques are available in the literature for addressing the stability problem of time delayed LFC systems [15-27], and references therein.

This paper investigates the impact of time delays on the stability of the two area LFC system integrated with an electric vehicle aggregator (EVA) loop. Integration of EVs to the grid is becoming a promising tool for frequency control and power grid stability. In this paper, using a novel Lyapunov-Krasovskii (LK) functional based analysis, delay-dependent stability is ascertained for EV integrated LFC system with dissimilar time-delays in the EVA loops.

2. TWO AREA LFC WITH EVAs

In a networked power system with signal transmission through communication channels, time delays are common and can be attributed to one of the following reasons: geographical displacement of the control and power source [9], cyber-attacks [10] or predominantly due to usage of open communication networks [8]. In the existing literature regarding two area LFC system with EVA loops, it is a usual practice that delays in the feedback loops are considered equal and combined as single delay while analysing the delay dependent stability of the system. But, the delays in the two EVA loops maybe different. The incommensurate time-delays in the EVA loops appears to be a more practical and realistic approach for addressing the stability problem in LFC-EVA systems [33-39].

Fig. 1 shows a networked control system, which has sensors, controllers, and actuators all connected via a communication network [9]. As the communication network is assumed to be completely dependable with a dedicated line for thermal or hydro power plants in typical power system studies, the effects of these delays on the system performance and

stability are not evaluated. A dedicated communication channel for each EV and distributed EV agent is not a feasible solution. Implementing communication across a general-purpose network (such as a wireless network or Ethernet/LAN/Internet) is the more practical option.
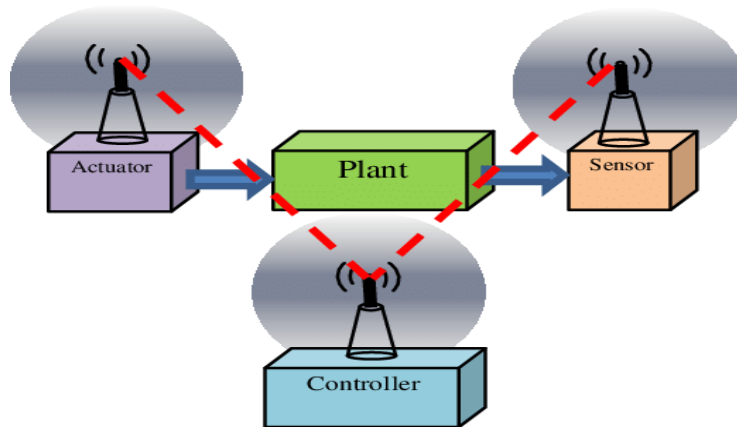
Fig. 1. Networked control system structure.

Fig. 2 presents the typical architecture of EVA integrated LFC system [9]. As seen from the figure, the concept of EVA employs hierarchical approach to control charging and discharging patterns of EVs. Generally, it is neither essential nor practically feasible for the control center to transmit the control signals to each and every EV individually. Hence, a fleet of EVs is integrated and considered as a wholesome unit called EVA. The function of EVA is the transmission of status information of a cluster of EVs assigned under it to the control center.
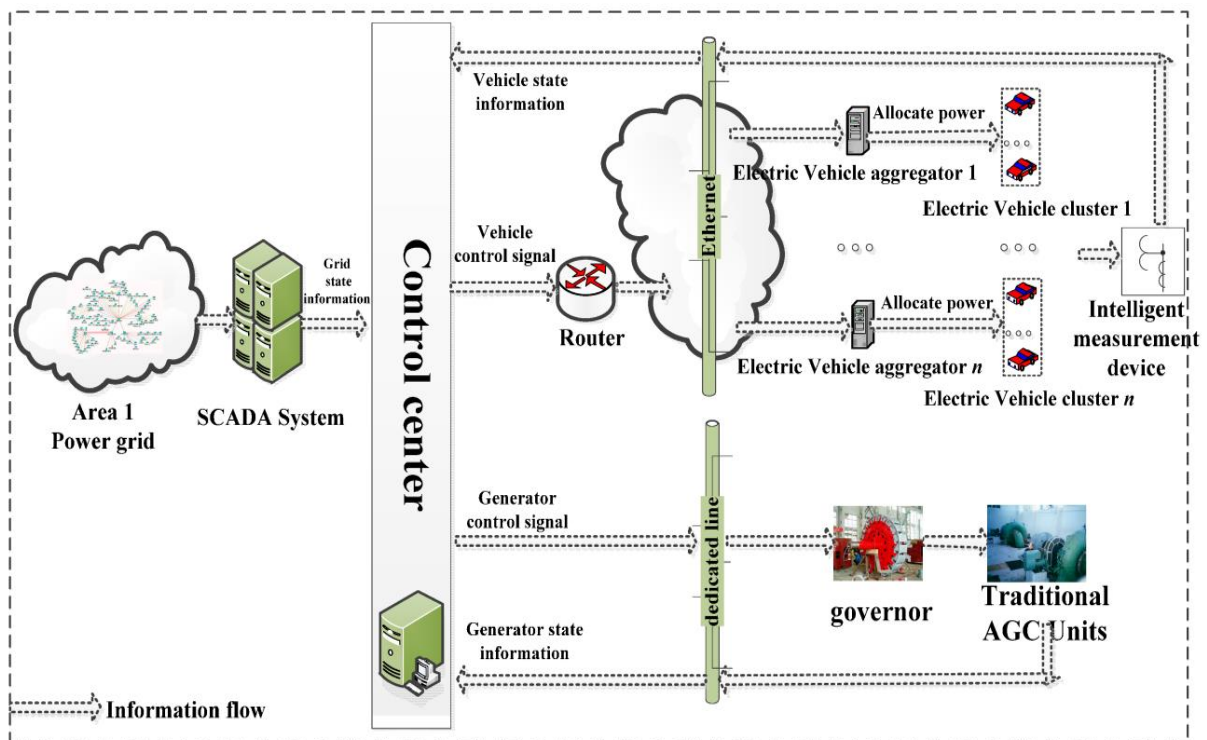
Fig. 2. Typical architecture of LFC system integrated with EVAs.

The supervisory control and data acquisition (SCADA) system sends the measured real time signals like frequency, tie line powers, etc., to the control center where area control center error is calculated. The control center receives the generating unit status and vehicle status. Based on the received real time signals, the control center sends the control signals to the generator and EVA. As observed from Fig. 2, the information flow from the control center to the generator is a dedicated communication channel, while that of control center to EVA and from EVA to EVs is an open communication network, which introduces time delays. Further, EVA sends the signals relating to the allocation of power to EVs cluster.

Fig. 3 presents the two-area closed loop LFC block diagram integrated with EVAs [5]. It is assumed that only a single EVA is present in each area, and all the EVs along with generators are lumped as equivalent modules under single EVA management. The notation used in Fig. 3 is given in Table 1.

The two-area LFC system with dissimilar time-delays in the EVA loops as shown in Fig. 2 is modelled in the following autonomous state-space framework:

$$\dot{x}(t) = Ax(t) + A_1 x(t - \tau_1) + A_2 x(t - \tau_2) \tag{1}$$

$$x(0) = \Phi(t), \tag{2}$$

where $x(t) \in R^{13 \times 1}$ is the state vector, and $A \in R^{13 \times 13}$, $A_1 \in R^{13 \times 13}$ and $A_2 \in R^{13 \times 13}$ are the system matrices (given in Appendix A) associated with current state vector and delayed state vectors. The initial condition $\Phi(t)$ is presented for $t \in \sim[-\max(\tau_1, \tau_2), 0]$.
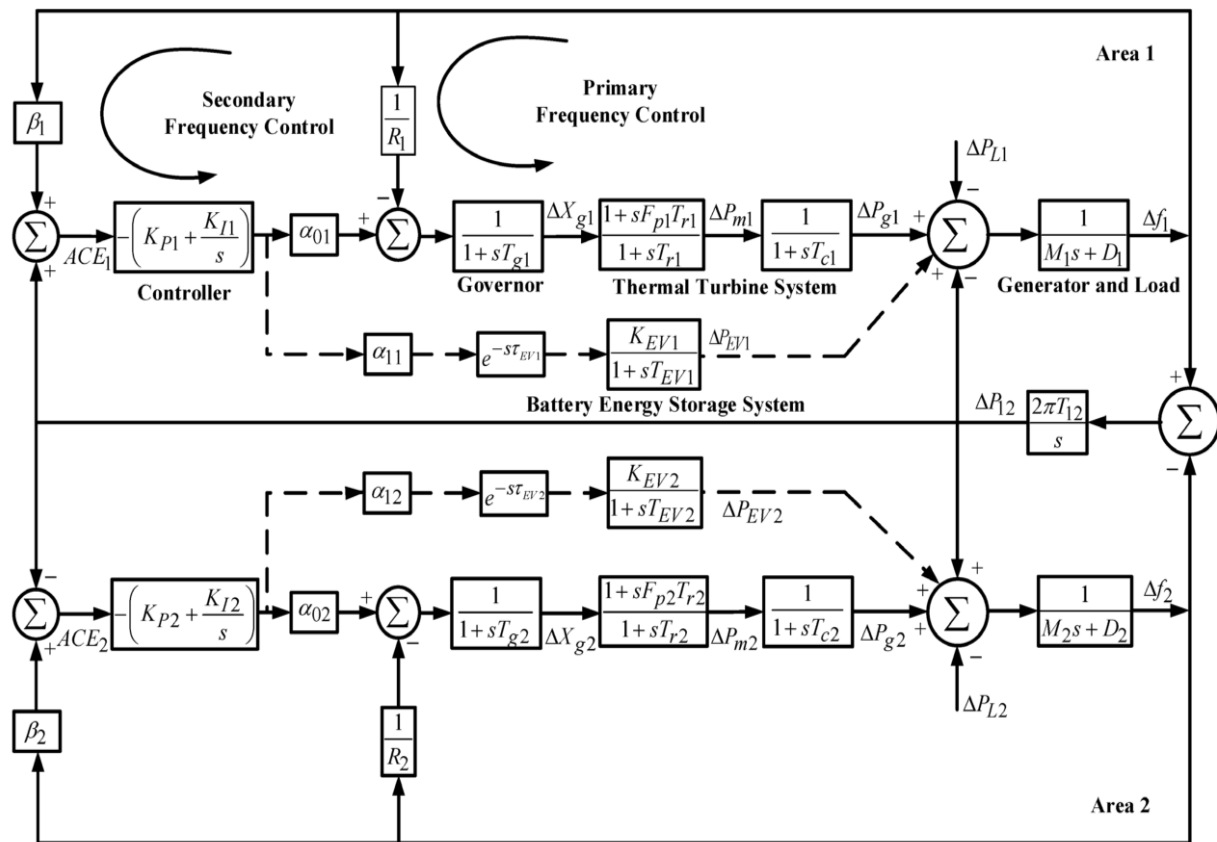
Fig. 3. Two-area LFC-EV system.

Table 1. Notations used in Fig. 3.

Notation	Nomenclature
ΔP_g	Generator power output
ΔP_m	Mechanical power output
ΔP_{EV}	The power output of EVA
D	Damping coefficient
R	Speed regulation coefficient
β	Frequency bias factor
F_p	Fraction of the turbine power
T_c	Turbine time constant
T_r	Reheat turbine time constant
T_g	Governor time constant
M	Inertia constant of generator
T_{EV}	Time constant of EVA
K_{EV}	Gain of EVA
K_P	Proportional gain of PI Controller
K_I	Integral gain of PI Controller
α_0	Participation factor of conventional generation
α_1	Participation factor of EVA
τ_1	Time-delay in EVA in area 1
τ_2	Time-delay in EVA in area 2
τ_d	Time-delay margin
θ	Angle between the two time-delays

3. STABILITY CRITERION

For deriving the stability criterion for assessing the delay dependent-stability of system in Eq. (1) subjected to Eq. (2), the following lemmas are required.

Lemma 1 - Jenson Integral Inequality [40]: For any positive symmetric constant matrix $M \in R^{nxn}$, scalars $r_1 < r_2$ and a vector valued function $\omega: [r_1, r_2] \rightarrow R^n$, the following inequality holds:

$$\left(\int_{r_1}^{r_2} \omega(s)ds \right)^T M \left(\int_{r_1}^{r_2} \omega(s)ds \right) \leq (r_2 - r_1) \int_{r_1}^{r_2} \omega^T(s) M \omega(s) ds \tag{3}$$

Lemma 2 - Wirtinger Inequality [41]: For a given symmetric positive definite matrix R and for any differentiable signal ω in $[a, b] \rightarrow R^n$, the following inequality holds:

$$\int_b^a \dot{\omega}^T(u) R \dot{\omega}(u) du \geq \frac{1}{b-a} \begin{bmatrix} \omega(b) \\ \omega(a) \\ \frac{1}{b-a}\int_a^b \omega(u)du \end{bmatrix}^T \begin{bmatrix} 4R & 2R & -6R \\ * & 4R & -6R \\ * & * & 12R \end{bmatrix} \begin{bmatrix} \omega(b) \\ \omega(a) \\ \frac{1}{b-a}\int_a^b \omega(u)du \end{bmatrix} \tag{4}$$

The proposed delay-dependent stability criterion for the system in Eq. (1) is presented in the form of the following theorem:

Theorem 1: The system in Eq. (1) with two non-identical time-invariant delays τ_1 and τ_2 is asymptotically stable in the sense of Lyapunov, if there exists real symmetric positive definite matrices $P_{11}, S_1, S_2, R_1, R_2$ and R_3, symmetric matrices P_{22} and P_{33}, free matrices P_{12}, P_{13} and P_{23} of appropriate dimensions such that the following linear matrix inequalities (LMIs) hold:

$$\Pi_0 > 0 \quad, \tag{5}$$

$$\begin{bmatrix} \sum_{k=1}^{5} \Pi_k & \bar{A}^T U_1 & \bar{A}^T U_2 \\ * & -U_1 & 0 \\ * & * & -U_2 \end{bmatrix} < 0 \tag{6}$$

where $\Pi_0 = P + diag([0, \tau_1^{-1} S_1, \tau_2^{-1} S_2])$, $\Pi_1 = \Phi_1^T P \Phi_2 + (\Phi_1^T P \Phi_2)^T$,

$\Pi_2 = diag([S_1 + S_2, -S_1, -S_2, 0, 0])$,

$$\Pi_3 = \begin{bmatrix} -\frac{4}{\tau_1} R_1 & -\frac{2}{\tau_1} R_1 & 0 & \frac{6}{\tau_1} R_1 & 0 \\ * & -\frac{4}{\tau_1} R_1 & 0 & \frac{6}{\tau_1} R_1 & 0 \\ * & * & 0 & 0 & 0 \\ * & * & * & -\frac{12}{\tau_1} R_1 & 0 \\ * & * & * & * & 0 \end{bmatrix}, \Pi_4 = \begin{bmatrix} -\frac{4}{\tau_2} R_2 & 0 & -\frac{2}{\tau_2} R_2 & 0 & \frac{6}{\tau_2} R_2 \\ * & 0 & 0 & 0 & 0 \\ * & * & -\frac{4}{\tau_2} R_2 & 0 & \frac{6}{\tau_2} R_2 \\ * & * & * & 0 & 0 \\ * & * & * & * & -\frac{12}{\tau_2} R_2 \end{bmatrix},$$

$\Pi_5 = [0 \quad I \quad -I \quad 0 \quad 0]^T (-R_{12}) [0 \quad I \quad -I \quad 0 \quad 0].$

with $P = \begin{bmatrix} P_{11} & P_{12} & P_{13} \\ * & P_{21} & P_{22} \\ * & * & P_{33} \end{bmatrix}$, $\Phi_1 = \begin{bmatrix} I & 0 & 0 & 0 & 0 \\ 0 & 0 & 0 & \tau_1 & 0 \\ 0 & 0 & 0 & 0 & \tau_2 \end{bmatrix}^T$, $\Phi_2 = \begin{bmatrix} A & A_1 & A_2 & 0 & 0 \\ I & -I & 0 & 0 & 0 \\ I & 0 & -I & 0 & 0 \end{bmatrix}$,

$\bar{A} = [A \quad A_1 \quad A_2 \quad 0 \quad 0]$, $U_1 = \tau_1 R_1 + \tau_2 R_2$, $U_2 = (\tau_2 - \tau_1)^2 R_{12}$.

Proof: The theorem is derived using the Lyapunov Krasovskii functional

$V(x(t)) = \sum_{i=1}^{4} V_i(x(t))$ with

$$V_1(x(t)) = \Xi^T(t) P \Xi(t) \tag{7}$$

$$V_2(x(t)) = \sum_{i=1}^{2} \int_{t-\tau_i}^{t} x^T(s) S_i x(s) ds \tag{8}$$

$$V_3(x(t)) = \sum_{i=1}^{2} \int_{-\tau_i}^{0} \int_{t+\theta}^{t} \dot{x}^T(s) R_i \dot{x}(s) ds d\theta \tag{9}$$

$$V_4(x(t)) = (\tau_2 - \tau_1) \int_{-\tau_2}^{-\tau_1} \int_{t+\theta}^{t} \dot{x}^T(s) R_3 \dot{x}(s) ds d\theta \tag{10}$$

with $\Xi(t) = \begin{bmatrix} x^T(t) & \int_{t-\tau_1}^{t} x^T(s) ds & \int_{t-\tau_2}^{t} x^T(s) ds \end{bmatrix}^T$

By Jenson's integral inequality, the following conditions hold:

$$\int_{t-\tau_1}^{t} x^T(s) S_1 x(s) ds \geq \left[\int_{t-\tau_1}^{t} x(s) ds \right]^T \left(\frac{S_1}{\tau_1} \right) \left[\int_{t-\tau_1}^{t} x(s) ds \right] \tag{11}$$

$$\int_{t-\tau_2}^{t} x^T(s) S_2 x(s) ds \geq \left[\int_{t-\tau_2}^{t} x(s) ds \right]^T \left(\frac{S_2}{\tau_2} \right) \left[\int_{t-\tau_2}^{t} x(s) ds \right] \tag{12}$$

Using Eqs. (11) and (12), a lower bound for $V(x(t))$ can be readily obtained as follows:

$$V(x(t)) \geq \Xi(t)^T \Pi_0 \Xi(t) + V_3(x(t)) + V_4(x(t) \tag{13}$$

Now, it is clear that the positive definiteness of the matrices $S_i, R_j; i = 1,2 \ and \ j = 1,2,3$ and $\Pi_0 > 0$ implies positive definiteness of $V(x(t))$.

The time derivative of the functional $V_1(x(t))$ along the trajectory of Eq. (2) is given by:

$$\dot{V}_1(x(t)) = 2 \Xi^T(t) P \dot{\Xi}(t) \tag{14}$$

which can be rewritten as

$$\dot{V}_1(x(t)) = \delta^T(t) \Pi_1 \delta(t) \tag{15}$$

where $\delta(t) = \begin{bmatrix} x^T(t) & x^T(t - \tau_1) & x^T(t - \tau_2) & \frac{1}{\tau_1} \int_{t-\tau_1}^{t} x^T(s) ds & \frac{1}{\tau_2} \int_{t-\tau_2}^{t} x^T(s) ds \end{bmatrix}^T$ is an augmented state vector.

The time-derivative of the functional $V_2(x(t))$ along Eq. (2) is given by

$$\dot{V}_2(x(t)) = x^T(t)(S_1 + S_2)x(t) - \sum_{i=1}^{2} x^T(t - \tau_i)S_i x(t - \tau_i) \qquad (16)$$

Eq. (16), in terms of $\delta(t)$, is expressed as follows:

$$\dot{V}_2(x(t)) = \delta^T(t)\Pi_2\delta(t) \qquad (17)$$

The time-derivative of the functional $V_3(x(t))$ along Eq. (2) is given by

$$\dot{V}_3(x(t)) = \dot{x}^T(t)U_1\dot{x}(t) - \int_{t-\tau_1}^{t} \dot{x}^T(s)R_1\dot{x}(s)ds - \int_{t-\tau_2}^{t} \dot{x}^T(s)R_2\dot{x}(s)ds \qquad (18)$$

Now, using Wirtinger inequality, Eq. (18) is expressed as inequality as follows:

$$\dot{V}_3(x(t)) \le \delta^T(t)(\bar{A}^T U_1 \bar{A})\delta(t) + \delta^T(t)\Pi_3\delta(t) + \delta^T(t)\Pi_4\delta(t) \qquad (19)$$

The time-derivative of $V_4(x(t))$ along Eq. (2) is given by

$$\dot{V}_4(x(t)) = \dot{x}^T(t)U_2\dot{x}(t) - (\tau_2 - \tau_1)\int_{t-\tau_2}^{t-\tau_1} \dot{x}^T(s)R_{12}\dot{x}(s)ds \qquad (20)$$

Now, using Jenson's integral inequality, Eq. (20) is expressed as an inequality as follows:

$$\dot{V}_4(x(t)) \le \delta^T(t)(\bar{A}^T U_2 \bar{A})\delta(t) + \delta^T(t)\Pi_5\delta(t) \qquad (21)$$

By combining the time-derivative of the LK functionals $\dot{V}(x(t)), i = 1\ to\ 4$, we get the following condition:

$$\dot{V}(x(t)) = \sum_{i=1}^{4}\dot{V}_i(x(t)) \le \delta^T(t)\left[\sum_{k=1}^{5}\Pi_k + \bar{A}^T(U_1 + U_2)\bar{A}\right]\delta(t) \qquad (22)$$

Now, by Schur Complement, if the inequality conditions in Eqs. (3) and (4) hold simultaneously, then there exists a sufficiently small scalar $\alpha > 0$ such that $\dot{V}(x(t)) \le -\alpha||x(t)||^2$, which - in turn - implies that the LFC systems described by Eq. (1) are asymptotically stable in the sense of Lyapunov [24]. Using the Lyapunov stability criterion in LMI framework, the delay margin values for the two area LFC system with EVAs are obtained.

4. RESULTS AND DISCUSSION

The nomenclature of the symbols used in the analysis is presented in Table 1, and the system parameters are given in Table 2. The stable delay margin values obtained using the Lyapunov stability criterion are listed in Tables 3 to 7 for different subsets of the PI controller parameters (K_p and K_I). In these tables, the multiple time delays are expressed as $\tau_d = \sqrt{\tau_1^2 + \tau_2^2}\ and\ \theta = tan^{-1}\left(\frac{\tau_2}{\tau_1}\right)$. The controller parameters in both of the control areas are assumed to be similar, i.e., $K_{p1} = K_{p2} = K_p$ and $K_{i1} = K_{i2} = K_i$. Hence, K_p and K_i are used to represent the parameters of the PI controller of both control areas. The participation factors are called otherwise as load sharing ratios between different generating units in a control area. The summation of the participation factors of the generating units in a control area should be unity at all times. In this under study system, conventional power generation and EVA are the two generating units in a control area. Therefore, the relation between their participation factors is given as $\alpha_0 + \alpha_1 = 1$.

For the purpose of analysis, two different scenarios are considered for two area LFC-EV systems. In scenario 1, the parameters in each control area are considered to be similar and hence, parameters of the control area 1 are the same as those of control area 2. In scenario 2, the parameters in each control area are considered to be dissimilar and hence, there exists two different sets of parameters for control area 1 and 2.

Table 2. Parameters under study for scenario 1.

Parameter	Area 1	Area 2
M	8.8	8.8
D	1	1
F_p	1/6	1/6
R	1/11	1/11
B	21	21
T_g	0.2	0.2
T_c	0.3	0.3
T_r	12	12
T_{EV}	0.1	0.1
K_{EV}	1	1
T_{12}	0.12	

For computing the stable delay margin, the proportional gain K_p is varied from 0.4 to 1.0 in steps of 0.2, and the integral gain K_i is set as 0.2 and 0.4. Table 3 presents the various cases considered for the delay margin computation of the system under study. Tables 4 and 5 present the delay margin values provided by the proposed stability criterion for various values of K_P and K_i of LFC controller with participation factor α_0= 0.8 and α_1=0.2. Tables 6 and 7 show the delay margin values for various values of K_p and K_i of LFC controller with participation factor α_0=0.7 and α_1=0.3.

Table 3. Cases considered for the delay margin computation of the investigated system.

Case	Scenario	K_i	α_0	α_1
1	1	0.4	0.8	0.2
2	1	0.6	0.8	0.2
3	1	0.4	0.7	0.3
4	1	0.6	0.7	0.3
5	2	0.4	0.7	0.3
6	2	0.6	0.7	0.3

Table 4. Delay margin results for K_i= 0.4, α_0=0.8 and α_1=0.2.

θ	K_p =0.4	K_p =0.6	K_p =0.8	K_p =1
5	1.836	2.028	2.027	1.913
10	1.872	2.060	2.056	1.939
20	2.004	2.183	2.167	2.039
30	2.243	2.433	2.389	2.229
40	2.346	2.671	2.678	2.514
45	2.272	2.567	2.585	2.455
50	2.346	2.671	2.678	2.514
60	2.243	2.433	2.389	2.229
70	2.004	2.183	2.167	2.039
80	1.872	2.060	2.056	1.939
85	1.836	2.028	2.027	1.913

Table 5. Delay margin results for K_i= 0.6, α_0=0.8 and α_1=0.2.

θ	K_p =0.4	K_p =0.6	K_p =0.8	K_p =1
5	1.053	1.300	1.424	1.447
10	1.074	1.320	1.443	1.466
20	1.154	1.396	1.520	1.540
30	1.324	1.552	1.668	1.681
40	1.331	1.718	1.886	1.905
45	1.314	1.681	1.880	1.896
50	1.331	1.718	1.886	1.905
60	1.324	1.552	1.668	1.681
70	1.154	1.396	1.520	1.540
80	1.074	1.320	1.443	1.466
85	1.053	1.300	1.424	1.447

Table 6. Delay margin results for K_i= 0.4, α_0=0.7 and α_1=0.3.

θ	K_p =0.4	K_p =0.6	K_p =0.8	K_p =1
5	1.393	1.501	1.452	1.331
10	1.415	1.521	1.470	1.347
20	1.499	1.601	1.544	1.413
30	1.674	1.755	1.681	1.535
40	1.839	1.986	1.904	1.734
45	1.791	1.956	1.905	1.758
50	1.839	1.986	1.904	1.734
60	1.674	1.755	1.681	1.535
70	1.499	1.601	1.544	1.413
80	1.415	1.521	1.470	1.347
85	1.393	1.501	1.452	1.331

Table 7. Delay margin results for K_i= 0.6, α_0=0.7 and α_1=0.3.

θ	K_p =0.4	K_p =0.6	K_p =0.8	K_p =1
5	0.867	1.046	1.108	1.089
10	0.880	1.059	1.122	1.102
20	0.932	1.114	1.178	1.155
30	1.037	1.220	1.282	1.255
40	1.132	1.384	1.455	1.419
45	1.122	1.380	1.471	1.451
50	1.132	1.384	1.455	1.419
60	1.037	1.220	1.282	1.255
70	0.932	1.114	1.178	1.155
80	0.880	1.059	1.122	1.102
85	0.867	1.046	1.108	1.089

The stable delay margins provided in Tables 9 and 10 are for different values of system parameters in area 1 and area 2. Another set of parameters of two area LFC systems with EVA is given in Table 8.

Table 8. Parameters under study for Scenario 2.

Parameter	Area 1	Area 2
M	8.8	6.6
D	1	0.8
F_p	1/6	0.15
R	1/11	0.085
B	21	20
T_g	0.2	0.45
T_c	0.3	0.25
T_r	12	10
T_{EV}	0.1	0.2
K_{EV}	1	0.8
T_{12}	0.12	

Table 9. Delay margin results for K_i= 0.4, α_0=0.7 and α_1=0.3.

θ	K_p =0.4	K_p =0.6	K_p =0.8	K_p =1
5	1.426	1.522	1.462	1.335
10	1.446	1.544	1.482	1.352
20	1.521	1.630	1.561	1.421
30	1.639	1.783	1.713	1.555
40	1.498	1.642	1.591	1.464
45	1.408	1.536	1.483	1.361
50	1.327	**1.437**	1.345	1.261
60	1.188	1.276	1.190	1.117
70	1.091	1.174	1.094	1.029
80	1.036	1.118	1.043	0.982
85	1.022	1.104	1.030	0.970

Table 10. Delay margin results for K_i= 0.6, α_0=0.7 and α_1=0.3.

θ	K_p =0.4	K_p =0.6	K_p =0.8	K_p =1
5	0.896	1.061	1.115	1.092
10	0.911	1.078	1.131	1.105
20	0.958	1.140	1.192	1.162
30	1.020	1.246	1.310	1.274
40	0.860	1.118	1.210	1.200
45	0.804	1.042	1.125	1.113
50	0.751	0.968	1.042	1.029
60	0.667	0.857	0.922	0.910
70	0.612	0.788	0.849	0.839
80	0.582	0.750	0.809	0.800
85	0.575	0.741	0.800	0.791

Using the time domain simulations, the analytical delay margin values are validated. The simulation studies are carried out for the LFC system to observe the evolution of the incremental frequency variable for various delay margin values when subjected to 0.1 p.u.

step load disturbance. From Table 9, considering scenario 2 (θ =50^0, K_p=0.6, K_I=0.4, α_0=0.7 and α_1=0.3), the value of delay margin corresponding to these parameters is τ_d=1.437 s.

Fig. 4 shows the marginally stable evolution of $\Delta f(t)$ for τ_d=1.437 s. It is observed that the system is on the verge of instability and the incremental frequency variable $\Delta f(t)$ exhibits sustained oscillation with respect to time. If delays are set at a value less than the stable delay margin, say τ_d= 1.4 s, the closed-loop system is asymptotically stable. For loop delays greater than the stable delay margin (simulation carried out for τ_d=1.5 s), the closed-loop system loses stability and $\Delta f(t)$ evolves unboundedly with time. Hence, the simulation results are in close agreement to the analytical results.
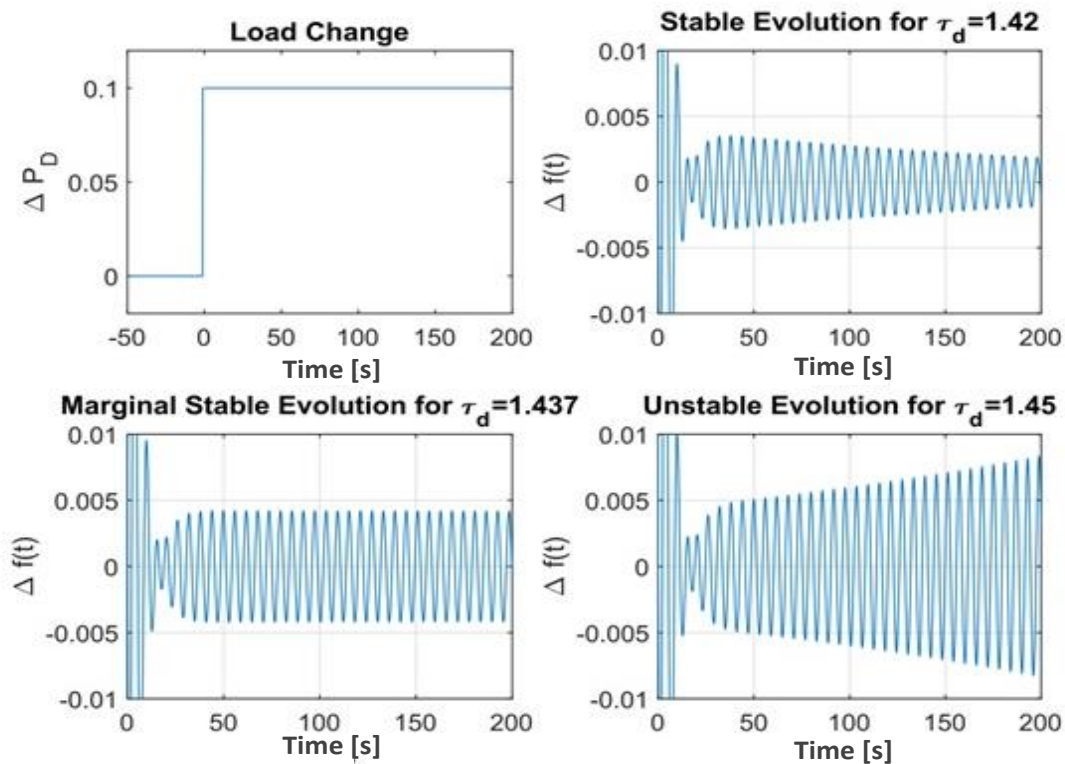
Fig. 4. Evolution of $\Delta f(t)$ for various values of delay for scenario 2.

5. CONCLUSIONS

In modern power systems, EVAs are integrated into the conventional system for improving dynamic performance. This paper assessed the impact of the time delays on the stability of networked two-area LFC-EV systems. The stable delay margin of LFC-EVA system was obtained for different sets of controller parameters and participation factors which helps in the optimal design of controllers for networked power systems. The possibility of extending the presented approach for the uncertain system with time-varying parametric uncertainties or exogenous noise will be explored in future works.

APPENDIX A: System Matrices of Two-Area LFC System with Dissimilar Time-Delays in the EVA Loops.

$$A = \begin{bmatrix}
\frac{-D_1}{M_1} & \frac{1}{M_1} & 0 & 0 & 0 & 0 & 0 & 0 & 0 & 0 & \frac{-1}{M_1} & \frac{1}{M_1} & 0 \\[4pt]
0 & \frac{-1}{Tc_1} & \frac{1}{Tc_1} & 0 & 0 & 0 & 0 & 0 & 0 & 0 & 0 & 0 & 0 \\[4pt]
\frac{-Fp_1}{R_1Tg_1}-\frac{Fp_1Kp_1\alpha_0\beta_1}{Tg_1} & 0 & \frac{-1}{Tr_1} & \frac{1}{Tr_1}-\frac{Fp_1}{Tg_1} & \frac{-Fp_1Ki_1\alpha_0}{Tg_1} & 0 & 0 & 0 & 0 & 0 & \frac{-Fp_1Kp_1\alpha_0}{Tg_1} & 0 & 0 \\[4pt]
\frac{-1}{R_1Tg_1}-\frac{Fp_1\alpha_0\beta_1}{Tg_1} & 0 & 0 & \frac{-1}{Tg_1} & \frac{-Ki_1\alpha_0}{Tg_1} & 0 & 0 & 0 & 0 & 0 & \frac{-Kp_1\alpha_0}{Tg_1} & 0 & 0 \\[4pt]
\beta_1 & 0 & 0 & 0 & 0 & 0 & 0 & 0 & 0 & 0 & +1 & 0 & 0 \\[4pt]
0 & 0 & 0 & 0 & 0 & \frac{-D_2}{M_2} & \frac{1}{M_2} & 0 & 0 & 0 & \frac{1}{M_2} & 0 & \frac{1}{M_2} \\[4pt]
0 & 0 & 0 & 0 & 0 & 0 & \frac{-1}{Tc_2} & \frac{1}{Tc_2} & 0 & 0 & 0 & 0 & 0 \\[4pt]
0 & 0 & 0 & 0 & 0 & \frac{-Fp_2}{R_2Tg_2}-\frac{Fp_2Kp_2\alpha_0\beta_2}{Tg_2} & 0 & \frac{-1}{Tr_2} & \frac{1}{Tr_2}-\frac{Fp_2}{Tg_2} & \frac{-Fp_2Ki_2\alpha_0}{Tg_2} & \frac{Fp_2Kp_2\alpha_0}{Tg_2} & 0 & 0 \\[4pt]
0 & 0 & 0 & 0 & 0 & \frac{-1}{R_2Tg_2}-\frac{Kp_2\alpha_0\beta_2}{Tg_2} & 0 & 0 & \frac{-1}{Tg_2} & \frac{-Ki_2\alpha_0}{Tg_2} & \frac{Kp_2\alpha_0}{Tg_2} & 0 & 0 \\[4pt]
0 & 0 & 0 & 0 & 0 & \beta_2 & 0 & 0 & 0 & 0 & -1 & 0 & 0 \\[4pt]
2piT_{12} & 0 & 0 & 0 & 0 & -2piT_{12} & 0 & 0 & 0 & 0 & 0 & 0 & 0 \\[4pt]
0 & 0 & 0 & 0 & 0 & 0 & 0 & 0 & 0 & 0 & 0 & \frac{-1}{TEV_1} & 0 \\[4pt]
0 & 0 & 0 & 0 & 0 & 0 & 0 & 0 & 0 & 0 & 0 & 0 & \frac{-1}{TEV_2}
\end{bmatrix}$$

$$A_1 = \begin{bmatrix}
0 & 0 & 0 & 0 & 0 & 0 & 0 & 0 & 0 & 0 & 0 & 0 & 0 \\
0 & 0 & 0 & 0 & 0 & 0 & 0 & 0 & 0 & 0 & 0 & 0 & 0 \\
0 & 0 & 0 & 0 & 0 & 0 & 0 & 0 & 0 & 0 & 0 & 0 & 0 \\
0 & 0 & 0 & 0 & 0 & 0 & 0 & 0 & 0 & 0 & 0 & 0 & 0 \\
0 & 0 & 0 & 0 & 0 & 0 & 0 & 0 & 0 & 0 & 0 & 0 & 0 \\
0 & 0 & 0 & 0 & 0 & 0 & 0 & 0 & 0 & 0 & 0 & 0 & 0 \\
0 & 0 & 0 & 0 & 0 & 0 & 0 & 0 & 0 & 0 & 0 & 0 & 0 \\
0 & 0 & 0 & 0 & 0 & 0 & 0 & 0 & 0 & 0 & 0 & 0 & 0 \\
0 & 0 & 0 & 0 & 0 & 0 & 0 & 0 & 0 & 0 & 0 & 0 & 0 \\
0 & 0 & 0 & 0 & 0 & 0 & 0 & 0 & 0 & 0 & 0 & 0 & 0 \\
0 & 0 & 0 & 0 & 0 & 0 & 0 & 0 & 0 & 0 & 0 & 0 & 0 \\
\frac{-KEV_1Kp_1\alpha_1\beta_1}{TEV_1} & 0 & 0 & 0 & \frac{-KEV_1Ki_1\alpha_1}{TEV_1} & 0 & 0 & 0 & 0 & 0 & \frac{-KEV_1Kp_1\alpha_1}{TEV_1} & 0 & 0 \\[4pt]
0 & 0 & 0 & 0 & 0 & 0 & 0 & 0 & 0 & 0 & 0 & 0 & 0
\end{bmatrix}$$

$$A_2 = \begin{bmatrix}
0 & 0 & 0 & 0 & 0 & 0 & 0 & 0 & 0 & 0 & 0 & 0 & 0 \\
0 & 0 & 0 & 0 & 0 & 0 & 0 & 0 & 0 & 0 & 0 & 0 & 0 \\
0 & 0 & 0 & 0 & 0 & 0 & 0 & 0 & 0 & 0 & 0 & 0 & 0 \\
0 & 0 & 0 & 0 & 0 & 0 & 0 & 0 & 0 & 0 & 0 & 0 & 0 \\
0 & 0 & 0 & 0 & 0 & 0 & 0 & 0 & 0 & 0 & 0 & 0 & 0 \\
0 & 0 & 0 & 0 & 0 & 0 & 0 & 0 & 0 & 0 & 0 & 0 & 0 \\
0 & 0 & 0 & 0 & 0 & 0 & 0 & 0 & 0 & 0 & 0 & 0 & 0 \\
0 & 0 & 0 & 0 & 0 & 0 & 0 & 0 & 0 & 0 & 0 & 0 & 0 \\
0 & 0 & 0 & 0 & 0 & 0 & 0 & 0 & 0 & 0 & 0 & 0 & 0 \\
0 & 0 & 0 & 0 & 0 & 0 & 0 & 0 & 0 & 0 & 0 & 0 & 0 \\
0 & 0 & 0 & 0 & 0 & 0 & 0 & 0 & 0 & 0 & 0 & 0 & 0 \\
0 & 0 & 0 & 0 & 0 & 0 & 0 & 0 & 0 & 0 & 0 & 0 & 0 \\
0 & 0 & 0 & 0 & 0 & \frac{-KEV_2Kp_2\alpha_1\beta_2}{TEV_2} & 0 & 0 & 0 & \frac{-KEV_2Ki_2\alpha_1}{TEV_2} & \frac{-KEV_2Kp_2\alpha_1}{TEV_2} & 0 & 0
\end{bmatrix}$$

REFERENCES

[1] H. Bevrani, *Robust Power System Frequency Control*, Springer, New York, 2009.

[2] P. Kundur, *Power System Stability and Control*, McGraw-Hill, New York, 1994.

[3] O. Elgerd, *Electrical Energy Systems Theory: An Introduction* , McGraw-Hill, 1971.

[4] H. Gündüz, S. Sönmez, S. Ayasun. "Comprehensive gain and phase margins based stability analysis of micro-grid frequency control system with constant communication time delays," *IET Generation, Transmission and Distribution*, vol. 11, no. 3, pp. 719-729, 2017.

[5] A. Naveed, S. Sönmez, S. Ayasun, "Identification of stability delay margin for load frequency control system with electric vehicles aggregator using Rekasius substitution," *2019 IEEE Milan PowerTech*, pp.1-6, 2019.

[6] A. Khalil, "Delay margin computation for load frequency control system with plug-in electric vehicles," *International Journal of Power and Energy Systems*, vol. 38, no. 3, pp. 1-17, 2018.

[7] S. Sönmez, S. Ayasun, C. Nwankpa, "An exact method for computing delay margin for stability of load frequency control systems with constant communication delays," *IEEE Transactions on Power Systems*, vol. 31, no. 1, pp. 370–377, 2016.

[8] S. Izadkhast, P. Garcia-Gonzalez, P. Frias, L. Ramirez-Elizondo, P. Bauer, "An aggregate model of plug-in electric vehicles including distribution network characteristics for primary frequency control," *IEEE Transactions on Power Systems*, vol. 31, no. 4, pp. 2987-2998, 2016.

[9] Y. Guo, L. Zhang, J. Zhao, F. Wen, A. Salam, J. Mao, L. Li, "Networked control of electric vehicles for power system frequency regulation with random communication time delay," *Energies*, vol. 10, no. 5, pp. 621,2017.

[10] A. Hajimiragha, C. Canizares, M. Fowler, S. Moazeni, A. Elkamel, "A robust optimization approach for planning the transition to plug-in hybrid electric vehicles," *IEEE Transactions on Power Systems*, vol. 26, no. 4, pp. 2264–2274, 2011.

[11] J. Yang, H. Dong, Y. Huang, L. Cai, F. Gou, Z. He, "Coordinated optimization of vehicle-to-grid control and load frequency control by considering statistical properties of active power imbalance," *International Transactions on Electrical Energy Systems*, vol. 29, no. 3, pp. e2750, 2019.

[12] A. Carreiroa, H. Jorgea, C. Antunesa, "Energy management systems aggregators: a literature survey," *Renewable Sustainable Energy Reviews*, vol. 73, pp. 1160-1172, 2017.

[13] L. Pekař, Q. Gao, "Spectrum analysis of LTI continuous-time systems with constant delays: a literature overview of some recent results," *IEEE Access*, vol. 6, pp. 35457-35491, 2018.

[14] K. Liu, A. Seuret, Y. Xia, F. Gouaisbaut, Y. Ariba, "Bessel-Laguerre inequality and its application to systems with infinite distributed delays," *Automatica*, vol. 109, pp. 108562, 2019.

[15] C. Zhang, Y. He, L. Jiang, M. Wu, H. Zeng, "Delay-variation-dependent stability of delayed discrete-time systems," *IEEE Transactions on Automatic Control*, vol. 61, no. 9, pp. 266-2669, 2016.

[16] C. Zhang, F. Long, Y. He, W. Yao, L. Jiang, M. Wu, "A relaxed quadratic function negative-determination lemma and its application to time-delay systems," *Automatica*, vol. 113, 2020.

[17] H. Zeng, Z. Zhai, Y. He, K. Teo, W. Wang, "New insights on stability of sampled-data systems with time-delay," *Applied Mathematics and Computation*, vol. 374, pp. 125041, 2020.

[18] H. Zeng, W. Liu, "A generalized free-matrix-based integral inequality for stability analysis of time-varying delay systems," *Applied Mathematics and Computation*, vol. 354, pp. 1-8, 2019.

[19] A. Seuret, F. Gouaisbaut, "Hierarchy of LMI conditions for the stability analysis of time-delay systems," *Systems and Control Letters* , vol. 81, no. 1, pp. 1-7, 2015.

[20] W. Yao, L. Jiang, Q. Wu, J. Wen, S. Cheng, "Wide-area damping controller of FACTS devices for inter-area oscillations considering communication time delays," *IEEE Transactions on Power Systems*, vol. 29, no. 1, pp. 318-329, 2014.

[21] L. Jin, C. Zhang, Y. He, L. Jiang, M. Wu, "Delay-dependent stability analysis of multi-area load frequency control with enhanced accuracy and computation efficiency," *IEEE Transactions on Power Systems*, vol. 34, no. 5, pp. 3687-3696, 2019.

[22] J. Thangaiah, R. Parthasarathy, "Delay-dependent stability analysis of microgrid with constant and time-varying communication delays," *Electric Power Components and Systems*, vol. 44, no. 13, pp. 1441-1452, 2016.

[23] A. Bilh, K. Naik, R. El-Shatshat, "Evaluating electric vehicles' response time to regulation signals in smart grids," *IEEE Transactions on Industrial Informatics*, vol. 14, no. 3, pp. 1210-1219, 2018.

[24] K. Gu, V. Kharitonov, J. Chen, *Stability of Time Delay Systems*, New York: Birkhauser, 2003.

[25] K. Walton, J. Marshall, "Direct method for TDS stability analysis," *IEE Proceedings D-Control Theory and Applications*, vol. 34, no. 2, pp. 101-107, 1987.

[26] Z. Rekasius, "A stability test for systems with delays," *Proceedings of Joint Automatic Control Conference*, no. 7, pp. 39, 1980.

[27] I. Delice, R. Sipahi, "Delay-independent stability test for systems with multiple time-delays," *IEEE Transactions on Automatic Control*, vol. 57, no. 4, pp. 963-972, 2012.

[28] C. Wu, F. Wen, Y. Lou, F. Xin, "Probabilistic load flow analysis of photovoltaic generation systems with plug-in electric vehicles," *International Journal of Electrical Power and Energy Systems*, vol. 64, pp. 1221–1228, 2015.

[29] T. Masuta, A. Yokoyama, "Supplementary load frequency control by use of a number of both electric vehicles and heat pump water heaters," *IEEE Transactions on Smart Grid*, vol. 3, pp. 1253–1262, 2012.

[30] M. Singh, P. Kumar, I. Kar, "Implementation of vehicle to grid infrastructure using fuzzy logic controller," *IEEE Transactions on Smart Grid*, vol. 3, pp. 565–577, 2012.

[31] O. Sundstrom, C. Binding, "Flexible charging optimization for electric vehicles considering distribution gridconstraints," *IEEE Transactions on Smart Grid*, vol. 3, pp. 26–37, 2012.

[32] M. Galus, S. Koch, G. Andersson, "Provision of load frequency control by PHEVs, controllable loads and acogeneration unit," *IEEE Transactions on Industrial Electronics*, vol. 58, no. 10, pp. 4568–4582, 2011.

[33] T. Yodyium, C. Mo-Yuen, "Control methodologies in networked control systems," *Control Engineering Practice*, vol. 11, no. 10, pp. 1099–1111, 2003.

[34] M. Cloosterman, N. Van de Wouw, W. Heemels, H. Nijmeijer, "Stability of networked control systems with uncertain time-varying delays," *IEEE Transactions on Automatic Control*, vol. 21, pp. 84–89, 2001.

[35] S. Mullen, *Plug-In Hybrid Electric Vehicles as a Source of Distributed Frequency Regulation*, Ph.D. Thesis, University of Minnesota, Minneapolis, MN, USA, 2009.

[36] W. Yao, J. Zhao, F. Wen, Y. Xue, G. Ledwich, "A hierarchical decomposition approach for coordinated dispatch of plug-in electric vehicles," *IEEE Transactions on Power Systems*, vol. 28, no. 3, pp. 2768–2778, 2013.

[37] G. Wang, J. Zhao, F. Wen, Y. Xue, G. Ledwich, "Dispatch strategy of PHEVs to mitigate selected patterns of seasonally varying outputs from renewable generation," *IEEE Transactions on Smart Grid*, vol. 6, pp. 627–639, 2015.

[38] C. Lu, C. Liu, C. Wu, "Dynamic modeling of battery energy storage system and application to power system stability," *IEE Proceedings-Generation, Transmission and Distribution*, vol. 142, pp. 429–435, 1995.

[39] M. Takagi, K. Yamaji, H. Yamamoto, "Power system stabilization by charging power management of plug-inhybrid electric vehicles with LFC signal," *In Proceedings of the Vehicle Power and Propulsion Conference*, Tokyo, Japan, pp. 822-826, 2009.

[40] X. Zhu, G. Yang, "Jensen integral inequality approach to stability analysis of continuous-time systems with time-varying delay," *IET Control Theory and Applications*, vol. 2, no. 6, pp. 524–534, 2008.

[41] A. Sauret, F. Gouaisbaut, "On the use of Wirtinger inequalities for time-delay systems," *IFAC Proceedings Volumes*, vol. 45, no. 14, pp. 260-265, 2012.